ELSEVIER

Carbohydrate Research 281 (1996) 79–98

CARBOHYDRATE RESEARCH

# The aqueous solution structure of a lipoteichoic acid from *Streptococcus pneumoniae* strain R6 containing 2,4-diamino-2,4,6-trideoxy-galactose: evidence for conformational mobility of the galactopyranose ring

Roger A. Klein [a,*], Rudolf Hartmann [a], Heinz Egge [a], Thomas Behr [b], Werner Fischer [b]

[a] *Institut für Physiologische Chemie der Universität Bonn, Nussallee 11, D-53115 Bonn, Germany*
[b] *Institut für Biochemie der Medizinischen Fakultät der Universität Erlangen-Nürnberg, Fahrstrasse 17, D-91054 Erlangen-Nürnberg, Germany*

Received 16 May 1995; accepted 15 September 1995

**Abstract**

The 2D-NOESY spectra for the per-*N*-acetylated and the native lipoteichoic acid (LTA) oligomer from *Streptococcus pneumoniae* strain R6 clearly indicate a difference in conformation of the 2,4,6-trideoxy-galactopyranose ring. Whereas the 2,4-*N*-acetylated Gal24N adopts the usual $^4C_1$ chair conformation, the native 2-*N*-acetyl-4-amino Gal24N exhibits conformational mobility with comparable populations in the $^4C_1$ chair and $^5S_1$ skew conformations, as determined using MD simulation for the partial trisaccharide Me-β-D-Glc6P-(1 → 3)-α-D-Gal24N-[6-PC]-(1 → 4)-α-D-GalNAc and from the intra-ring NOE effects. $^{31}$P-NMR spectra point to a strong electrostatic or

Abbreviations: Gal24N, 2,4-diamino-2,4,6-trideoxy-D-galactopyranose; Glc, D-glucopyranose; Gal, D-galactopyranose; GalNAc, 2-acetamido-2-deoxy-D-galactopyranose; PC, phosphorylcholine; RibP, ribitol 5-phosphate; NMR, nuclear magnetic resonance; NOE, nuclear Overhauser enhancement; FABMS, fast atom bombardment mass spectrometry; TSP, sodium 4,4-dimethyl-4-silapentanoate-2,2′,3,3′-$d_4$; ABNR, adopted basis Newton–Raphson; CJ, conjugate gradient; SD, steepest descents; TPPI, time-proportional phase increment; TIP3, TIP3 water molecule; CHARMm, Chemistry at Harvard Molecular Mechanics force field; MM2, Allinger's Molecular Mechanics force field; MMX, extended version of MM2 from Serena Software; MCS, Monte Carlo simulation; $\Phi$, (H-1–C-1–O-1–C-X); $\Psi$, (C-1–O-1–C-X–H-X); $\Omega$, (O-1–C-6–C-5–O-5); r.m.s., root mean square; LTA, lipoteichoic acid

* Corresponding author. Tel: +49 228 73 2422; Fax: +49 228 23 7677.


*SSDI* 0008-6215(95)00336-3

hydrogen-bonding interaction between the free 4-$NH_2$ group on the Gal24N and the negatively charged diester phosphate group between adjacent pentasaccharide repeating-units [Ribitol-(5 → 6)-β-D-Glc6P]. Molecular modelling and MD simulation experiments confirmed that such an interaction was feasible with the Gal24N galactopyranose ring in the inverted $B_{1,4}$ or skew $^5S_1$ conformation.

*Keywords:* *Streptococcus pneumoniae*; Lipoteichoic acid; Ring conformation; 2,4,6-Trideoxy-galactose; Chair; Inverted boat, $B_{1,4}$; Skew, $^5S_1$; Computer modelling; NMR; NOE; MD simulation

## 1. Introduction

We have recently determined the structure and likely conformation in aqueous solution of the lipoteichoic acid (LTA) from *Streptococcus pneumoniae* strain R6 in the form of the per-*N*-acetylated oligomer ($n = 5–7$) and the isolated pentasaccharide repeating-unit, using NMR and computational methods [1]. The repeating-unit contains D-glucose, 2,4-diamino-2,4,6-trideoxy-galactose, and two *N*-acetylgalactosamine residues substituted at the 6-position by phosphorylcholine, as well as a ribitol residue linked, in the oligomer, to the 6-$PO_4$-glucose of the next repeating-unit. The per-*N*-acetylated oligomer was originally used for analytical reasons, in particular as a means of improving NMR resolution. The conformation of the Gal24N residue in the per-*N*-acetylated material was clearly the $^4C_1$ chair form, as evidenced by intra-ring NOE data and available coupling constants.

We also reported a marked effect on the $^{31}$P-NMR spectrum of having the Gal24N-4-$NH_2$ free, as in the native material, compared with that of the per-*N*-acetylated oligomer. The line-width of the $^{31}$P signal from the inter-residue phosphate was greatly broadened in the presence of the free $NH_2$ group, with small effects also being seen for the phosphorylcholine phosphate groups. No line broadening was observed with the isolated repeating-unit. We interpret these observations as indicating a strong interaction between the Gal24N-4-$NH_2$ group and the charged diester phosphate between the ribitol and glucose residues. The structure of the lipoteichoic acid and the postulated interaction between the amino and phosphate groups are shown diagrammatically in Schemes 1–3, which are not intended to be conformationally accurate. The 4-$NH_2$ group, which may be either *N*-acetylated or free, is shown marked with the asterisks (***).

In this paper we show, by comparing the 2D-NOESY spectra for the *N*-acetylated and native oligomer, as well as using MD simulations for a partial trisaccharide containing the glucose 6-phosphate and Gal24N residues, that the 2,4,6-trideoxy-galactopyranose ring undergoes a conformational transition between the $^4C_1$ chair and the inverted skew $^5S_1$ conformations, corresponding to approximately equal conformer populations at 300 K, only when the Gal24N-4-$NH_2$ group is free. When the 4-$NH_2$ group is *N*-acetylated the Gal24N ring remains exclusively in the $^4C_1$ chair conformation. The lipoteichoic acid oligomer is peculiarly suited to conformational analysis by NMR since the homogeneity of the repeat pentasaccharide is of a very high order, that is, there appears to be no substitution heterogeneity which might otherwise degrade spectral resolution.

The conformational flexibility of the iduronic acid (IdoA) ring, with the presence of

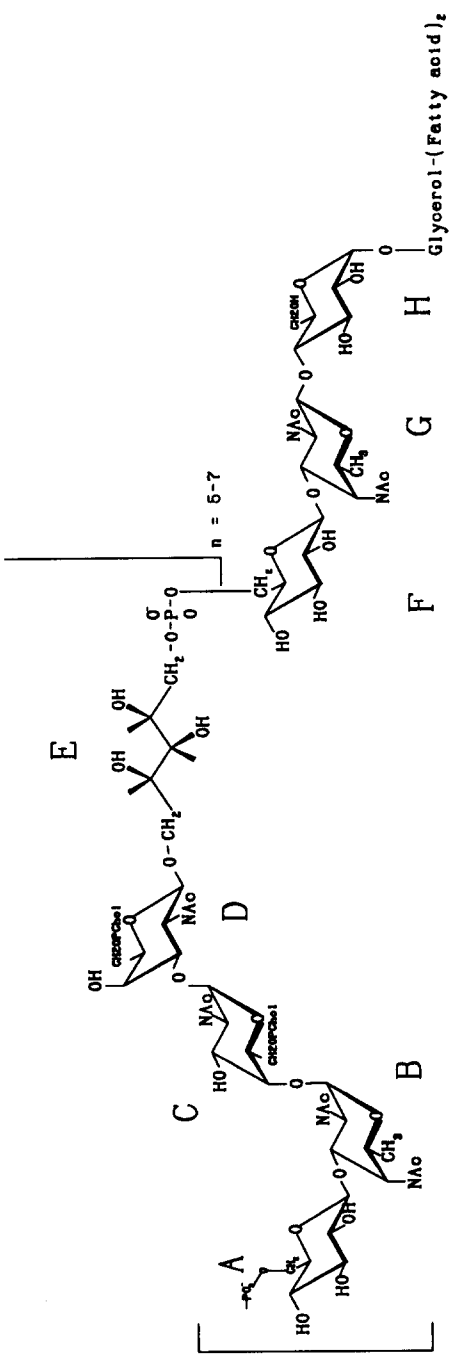


Scheme 1. The LTA oligomer from *Streptococcus pneumoniae* strain R6.

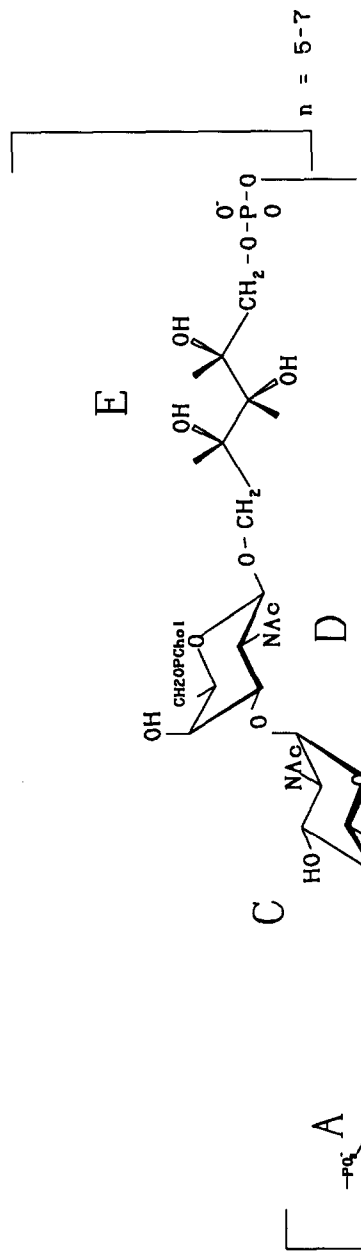


Scheme 2. The pentasaccharide repeating-unit from the LTA oligomer.

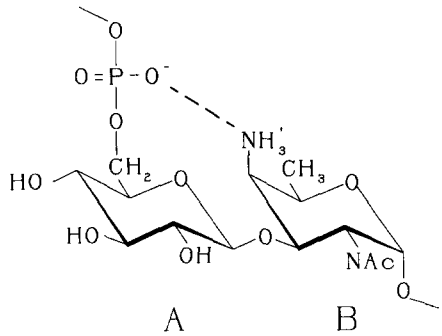


Scheme 3. Representation of the interaction between the 4-$NH_2$ group of Gal24N and the phosphate group 6-linked to the D-glucose residue and to the ribitol of the previous repeating-unit.

the preferred $^2S_O$ skew conformation, is possibly the best documented example in the literature of a non-rigid hexopyranose ring [2–9]. Extensive work has been done on the NMR and computer modelling of the IdoA residue in glycosaminoglycans (GAGs), especially heparin. A recent molecular dynamics study of the conformation of the iduronate ring by Forster and Mulloy [9] has shown extensive interconversion of the boat and skew conformers. In other cases most oligosaccharides found naturally contain hexopyranoses in the chair conformation, for example $^4C_1$ or $^2C_5$, as evidenced from coupling constant data [10,11].

Probable biological implications are discussed of this conformational equilibrium between the chair and skew forms, as well as the presence of permanently charged sugars at physiological pH. In particular we offer one possible explanation for the observations in the literature on the formation of abscesses by bacterial polysaccharides containing opposite charges, based on modulation of their antigenicity through conformational change.

## 2. Materials and methods

The oligomer attached to the 2-*O*-deacylated lipid anchor and the tetrasaccharide–ribitol repeating-unit were prepared from the *Streptococcus pneumoniae* strain R6 as described previously [1,12].

*NMR spectroscopy.*—NMR spectra were determined using a Bruker 500 MHz spectrometer and standard acquisition software. Samples were repeatedly exchanged against 99.96% $D_2O$ by freeze drying (at least $\times 3$). For measurement the sample was dissolved in 0.5 ml 99.96% $D_2O$ containing a small amount of sodium 4,4-dimethyl-4-silapentanoate-2,2′,3,3′-$d_4$ (TSP) as the shift reference ($\delta = 0.00$ ppm). Spectra were recorded at 298 K. 2D-NOESY experiments were carried out using the pulse sequence contained in the standard software, with mixing times satisfying the initial rate approximation (50–250 ms [1]). A matrix size of $2048 \times 512$ was used with 256 scans in TPPI mode, followed by zero-filling to $2048 \times 2048$ and processing with a phase-shifted sine

filter. After phase correction in F1 and symmetrisation, cross-peak volumes were determined using standard Bruker software.

The relationship between NOE cross-peak intensities and cross-relaxation rates has been derived for a pair of spin $\frac{1}{2}$ nuclei, showing through-space connectivity [13], with the cross-peak intensity an exponential function of the mixing time, $\tau_m$, in the large molecule limit. For short mixing times (the initial rate approximation) NOESY cross-peak intensities are directly proportional to cross-relaxation rates and thus to the inverse sixth power of the inter-proton distance, $r$ [14],

$$r_{ij}/r_0 = (a_0/a_{ij})^{1/6}$$

Reference cross-peak intensities and distances are available using the ring protons of the $^4C_1$ hexopyranoses or the $^2C_5$ conformer of neuraminic acid. For β-D-glucopyranosides and β-D-galactopyranosides the H-1–H-3, H-3–H-5, and H-1–H-5 protons are fixed at distances of approximately 2.50 Å [15], whereas for α-D-glucopyranosides and α-D-galactopyranosides the H-1–H-2 and H-3–H-5 proton pairs are 2.50 Å apart [16]. In the case of α-Neu5Ac residues, the proton pairs H-$3_{ax}$–H-5, H-$3_{eq}$–H-4, and H-4–H-6 provide reference distances of 2.50 Å [17]. Estimates of the cross-peak volume error, based on measurement reproducibility and peak overlap, gave uncertainties in the calculated distances of typically ±10% at ≥3.0 Å, with approximately ±5–7% at smaller distances. By using the H-3–H-4 distance in the Gal24N ring as an internal reference distance (see later), relative rather than absolute inter-proton distances were found to be more reproducible, usually ±3–5% or better. Absolute NOE-derived H–H distances, averaged over mixing times of 100–250 ms, however, were reproducible to within ±1–2%.

*Computational methods.*—The CHARMm force field [18] was used for all molecular mechanics and molecular dynamics calculations, in conjunction with the Quanta* user interface Version 4.0 (Molecular Simulations, Cambridge, UK). Atomic charges, determined by the Gasteiger method [19], were used. Starting structures and their coordinates were generated as previously described [1]. The unit charge carried by the phosphate and quaternary ammonium groups of the choline residue, as well as the other amino and phosphate groups, corresponds to a pH value around neutrality.

Computer calculations were carried out on a Silicon Graphics 150 MHz Indigo$^2$ XZ workstation. Reasonable starting geometries were obtained, using progressively disaccharides and then larger subunits, by minimisation with a geometrical, near-neighbour distance algorithm followed by at least 100 cycles of a steepest descent (SD) minimisation to remove any remaining bad contacts. Full minimisations were performed using the adopted-basis Newton–Raphson (ABNR) method, with a distance-dependent dielectric constant ($2r$) to simulate solvent water [18].

The $\Phi$ angle for a normal glycosidic linkage is defined by the torsional set H-1–C-1–O-1–C-X, where C-1 is the anomeric carbon and C-X the substituted carbon in the aglycon. The $\Psi$ angle is defined by the set H-X–C-X–O-1–C-1. In the case of a 6-linked residue an additional angle, $\Omega$, is defined by the set O-1–C-6–C-5–O-5. Ring torsional angles are defined in terms of the ring heavy atoms: tor1 = O-5–C-1–C-2–C-3; tor2 = C-1–C-2–C-3–C-4; tor3 = C-2–C-3–C-4–C-5; tor4 = C-3–C-4–C-5–O-5; tor5 = C-4–C-5–O-5–C-1; tor6 = C-5–O-5–C-1–C-2.

MD simulations were carried out at 300 K for either 1000 ps (1 ns) or 5000 ps (5 ns), unless otherwise stated, after 10 ps heating from 0 to 300 K followed by a short equilibration phase (10–20 ps) at 300 K, maintaining starting geometry. A 1 fs integration step was used and either 2000 or 5000 conformations stored for further analysis. Torsion and distance data were then analysed using commercially available software (Grapher, Golden Software, Colorado, and Statistica, Statsoft, Oklahoma).

Cremer–Pople ring-puckering parameters [20] were calculated from the Cartesian coordinates using RINGS, a FORTRAN program written in this laboratory for performing the necessary vector algebra [1]. This program determines connectivities and ring sizes based on known bond lengths, then calculates the Cremer–Pople parameters. It can be used on PCs and Unix workstations, such as the Silicon Graphics 4D25TG or Indigo[2]. Input data are contained as XYZ coordinates in an ASCII file.

## 3. Results and discussion

The evidence for a strong interaction between the Gal24N-4-$NH_2$ group, when free, i.e., non-acetylated, and the intra-chain diester phosphate is shown in Fig. 1. In this figure, line broadening of the $^{31}$P-NMR lines, especially for the $PO_4$ group between adjacent repeating-units, is seen only when the 4-$NH_2$ is not derivatised and there is a phosphate group attached to the 6-position of the glucose residue. The structures of the oligomer and the isolated repeating-unit are shown diagrammatically in Schemes 1 and 2, with a representation of the proposed electrostatic interaction between the amino and phosphate groups shown in Scheme 3.

The 2D-NOESY spectra for the per-*N*-acetylated oligomer and the native oligomer with free 4-$NH_2$ groups are compared in Fig. 2. The dotted lines joining corresponding cross-peaks in the two spectra, which are orthogonal to the diagonal, represent those cross-peaks whose chemical shifts in the F1 and F2 dimensions are not affected, or only minimally, by acetylation of the 4-$NH_2$ group. On the other hand the heavy lines, which are not at right angles to the diagonal, connect those cross-peaks exhibiting substantial substitution shifts, generally involving the ring protons of the Gal24N residue. Moreover, the cross-peak volumes for these H–H interactions, especially for those within the Gal24N hexopyranose ring-system itself, also show marked differences—highlighted by the rectangles—pointing to changes in the inter-proton distances.

The experimentally determined relative inter-proton distances for the Gal24N ring, with reference to the H-3–H-4 vector, are shown in Table 1 for the native oligomer, the per-*N*-acetylated oligomer, and the per-*N*-acetylated pentasaccharide repeating-unit. Irrespective of conformation, whether chair, boat, or skew, the H-3–H-4 distance remains relatively constant at $2.42 \pm 0.15$ Å, making it suitable for use as an internal reference, and within the experimental error of the NOE-derived distance measurements. Experimental values for the absolute H-3–H-4 distance in the native and per-*N*-acetylated oligomer were $2.56 \pm 0.05$ and $2.48 \pm 0.06$ Å, respectively, falling within these limits.

[1] Copies of the FORTRAN 77 source code are available to interested academic users from R.A. Klein.

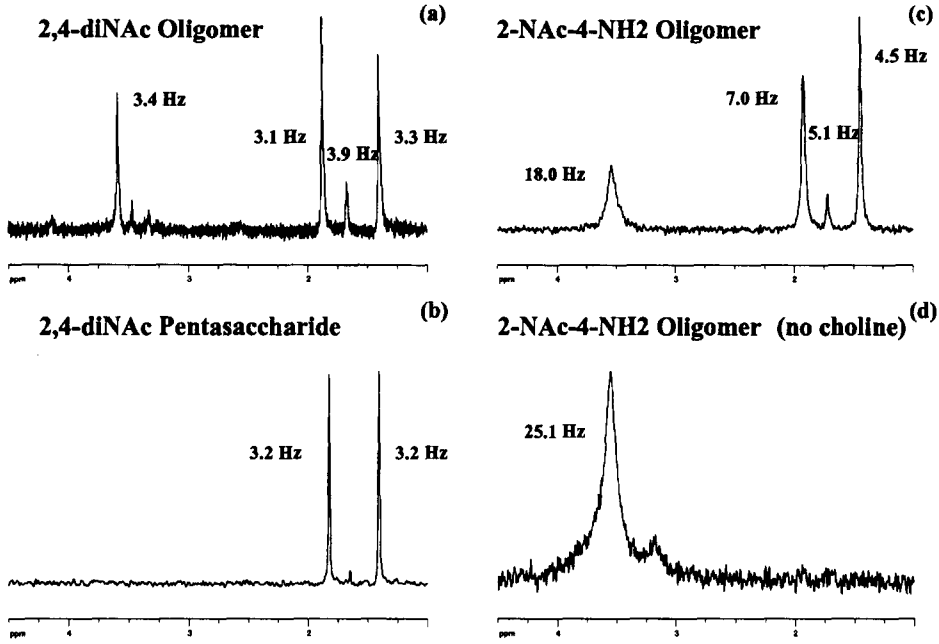


Fig. 1. $^{31}P$ spectra at 202.45 MHz for (a) the oligomer containing the 2,4-diNAc-2,4,6-trideoxy-2,4-diamino-galactopyranose unit (B); (b) the di-*N*-acetylated repeat pentasaccharide without the terminal $PO_4$ group; (c) the native oligomer with the 4-$NH_2$ group free; and (d) the native oligomer with the 4-$NH_2$ group free and the two choline groups removed. All chemical shifts are referenced to $Na_3PO_4$ as an internal standard at 6.0 ppm [referenced to 85% $H_3PO_4$ (Bruker)].

It is clear from the data in Table 1 that the Gal24N-H-5 proton moves further away, relatively and absolutely, from the H-3–H-4 vector when the 4-$NH_2$ group is not acetylated. The results for the per-*N*-acetylated oligomer and pentasaccharide repeat structure are indistinguishable, within experimental error. The H-3–H-5 inter-proton distance shows the greatest relative change of about +20%, compared to approximately +12% for the H-4–H-5 distance. The $^1$H-NMR 500 MHz chemical-shift assignments for the native oligomer (free 4-$NH_2$ groups; bold type) and the per-*N*-acetylated oligomer are shown in Table 2.

Such changes in the inter-proton distances can only be explained by considering different ring conformations. Apart from the stable $^4C_1$ chair conformation, other conformations such as boat or skew, or even the inverted chair $^1C_4$, are possible for hexopyranoses. The $^4C_1$ chair is usually the most stable for unsubstituted hexopyranoses, with the inverted $^1C_4$ chair being the least stable, that is, of highest energy. These energetic relationships between the $^4C_1$ chair, boat and skew forms are shown diagrammatically in Fig. 3, based on the work of Eliel [21]; the energy differences given in this figure are only indicative of the order of magnitude to be expected. The energy barriers between boat and skew forms are fairly low, usually of the order of a few kT (Boltzmann) units.

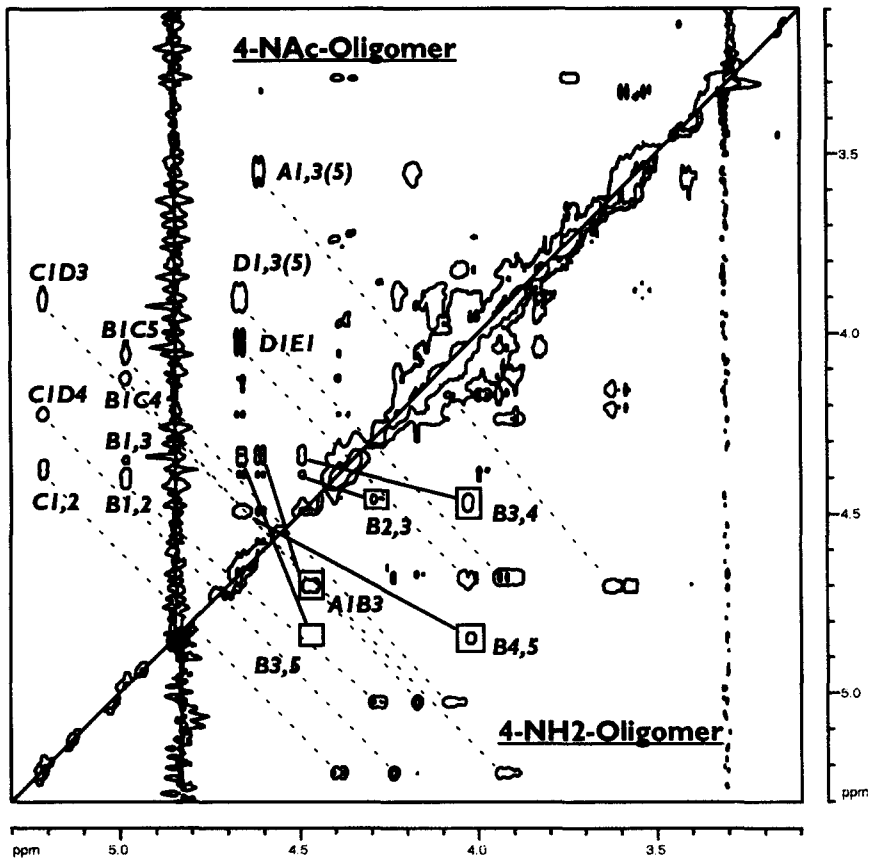


Fig. 2. The comparison of the 2D-NOESY spectrum for the 4-*N*-acetylated LTA oligomer (upper left) and the native LTA oligomer with free 4-$NH_2$ groups (lower right). The spectra shown were recorded with a mixing time of 250 ms; other conditions are given in Section 2. Both inter-residue (e.g., A1B3) and intra-residue [e.g., A1,3(5)] cross-peaks are shown, with dotted lines indicating equivalent peaks in the two spectra. The major differences for the cross-peaks associated with the B residue (Gal24N) are shown enclosed in rectangles for the 4-$NH_2$ oligomer, with solid lines indicating the equivalent peaks.

Table 1
Relative inter-proton distances within the hexopyranose ring of the B unit (Gal24N) using the H-3–H-4 distance as the reference ( = 1.00), determined from the integrated cross-peak volumes in the 2D-NOESY spectra

| Cross-peaks (NOE) | 2-NAc-4-$NH_2$ oligomer | 2,4-diNAc oligomer | 2,4-diNAc repeat pentamer |
|---|---|---|---|
| B1,2 | 0.92 ± 0.01 | 0.95 ± 0.03 | 0.96 |
| B3,4 | 1.00 | 1.00 | 1.00 |
| B4,5 | 1.04 ± 0.03 | 0.92 ± 0.01 | 0.94 |
| B3,5 | 1.25 ± 0.10 | 1.05 ± 0.01 | 1.06 |

Table 2
$^1$H 500 MHz Chemical-shift assignments for the phosphorylated pentasaccharide repeating-unit contained within the oligomer ($n = 5$–7). The values shown in bold type are for the native oligomer with a free 4-$NH_2$ group on the trideoxygalactose ring; values shown in normal type are for the per-*N*-acetylated oligomer (Klein et al. [1]). Asterisked values have limited accuracy due to the spectral resolution available

| Atom | Unit | | | | | | Choline | |
|---|---|---|---|---|---|---|---|---|
| | A′ | A | B | C | D | E | | |
| H-1 | **4.64** | **4.70** | **5.03** | **5.22** | **4.67** | **4.03** | **(C)** | |
| | 4.57 | 4.63 | 5.01 | 5.22 | 4.68 | 3.92<br>4.01 | **3.30** | ($CH_3N$) |
| H-2 | **3.42** | **3.40** | **4.28** | **4.39** | **4.17** | – | 3.30 | |
| | 3.39 | 3.34 | 4.40 | 4.39 | 4.18 | 4.06 | **4.36** | ($OCH_2$) |
| H-3 | – | **3.62** | **4.47** | **3.99** | **3.93** | – | 4.35 | |
| | – | 3.55 | 4.36 | 3.96 | 3.92 | 3.82 | **3.73** | ($NCH_2$) |
| H-4 | – | **3.60** | **4.02** | **4.17** | **4.24** | – | 3.74 | |
| | – | 3.61 | 4.51 | 4.14 | 4.23 | 3.95 | | |
| H-5 | – | **3.57** | **4.85** | **3.89** | **3.90** | – | **(D)** | |
| | – | 3.55 | 4.67 | 4.08 | 3.89 | 4.15 | **3.30** | ($CH_3N$) |
| H-6a | – | | **1.23** | **4.09*** | **4.14*** | – | 3.30 | |
| | – | 4.18 | 1.11 | 4.04 | 4.12 | | **4.41** | ($OCH_2$) |
| H-6b | – | | | | | | 4.39 | |
| | – | | ($CH_3$) | | | | **3.75** | ($NCH_2$) |
| H-6c | | | | | | | 3.75 | |

Calculations of the stabilities of the various ring conformers for an isolated 2-acetamido-4-amino-2,4,6-trideoxy-galactopyranose ring using the CHARMm force field, with dielectric constants between 1 and 80 as well as a distance-dependent value for the constant, showed the $^{1,4}B$ boat, the most stable conformer except for the $^4C_1$ chair, to be some 4–5 kcal/mol less stable that the $^4C_1$ chair, with this and the skew and inverted boat conformers being within 2–3 kcal/mol of one another.

When minimisation was carried out on the trisaccharide (II), in conjunction with MD experiments, it turned out that the $^5S_1$ form, a slightly skewed $B_{1,4}$ inverted boat in rapid equilibrium with the true inverted boat, was 3 kcal/mol more stable than the $^4C_1$ chair in terms of its enthalpy. Another less stable skewed boat form was also observed (see below). The stability of this $^5S_1$ skew compared to the $^4C_1$ chair is probably due to interactions between the 4-amino group, which is equatorial in both the $^5S_1$ and $B_{1,4}$ forms rather than axial as in the $^4C_1$ form, and the phosphate group, as well as through hydrogen bonding with the ring oxygen of the glucose residue, as evidenced by molecular modelling.

We have calculated Cremer–Pople parameters for the three hexopyranose rings in the minimised trisaccharide (II), using the program RINGS, with the Gal24N in either the chair, or the two skew conformations. The glucopyranose and 2-amino-2-deoxy-galactopyranose (galactosamine) rings gave nearly perfect values for $^4C_1$ chair geometry, i.e., for D-glucose $Q = 0.5708 \pm 0.0141$, $q_2 = 0.0388 \pm 0.0356$, $q_3 = 0.5695 \pm 0.0107$, with $\theta = 1$–$8°$, and for galactosamine $Q = 0.5710 \pm 0.0079$, $q_2 = -0.0167 \pm 0.0294$, $q_3 = 0.5699 \pm 0.0068$, with $\theta = 2$–$5°$, irrespective of the substitution and conformation of the Gal24N residue.

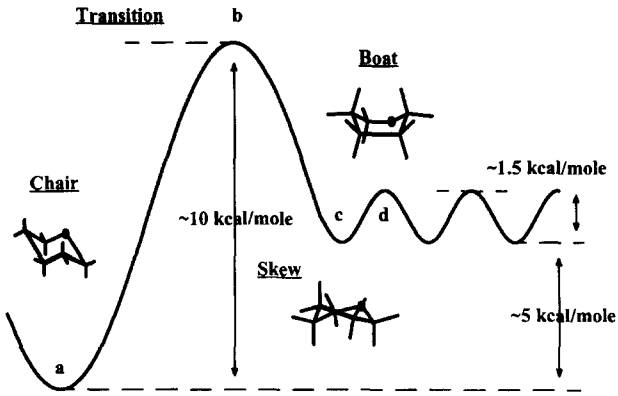


Fig. 3. Potential energy of a hexopyranose ring as a function of conformation. Adapted from data for cyclohexane given by Eliel [20]: (a) refers to the chair $^4C_1$ conformation, (b) to the transition state, (c) and (d) to the skew and boat conformations. The difference in potential energy between the stable $^4C_1$ chair conformation (a) and the skew and boat conformations [(c) and (d)], which are separated by 2–3 kcal/mol, is approximately 5–7 kcal/mol.

The chair form of Gal24N gives virtually identical results, $Q = 0.5805$, $q_2 = 0.004$, $q_3 = 0.5799$, with $\theta = 3°$, indicating undistorted $^4C_1$ geometry. On the other hand the stable $^5S_1$ conformer gives values typical of a skewed inverted boat, namely, $Q = 0.6954$, $q_2 = -0.6034$, $q_3 = 0.0393$, with $\theta = 87°$ and $\phi = 330°$. This conformer is not a "pure" inverted boat but is slightly distorted. The relatively high energy $^OS_2$ skew conformation possesses Cremer–Pople parameters as follows: $Q = 0.7126$, $q_2 = -0.0173$, $q_3 = 0.0752$, with $\theta = 84°$ and $\phi = 271°$. Both of these last two conformations lie near to the equator of the Cremer–Pople sphere ($\theta = 90°$) indicating boat or twisted-boat (skew) structures [9,21,22].

Forster and Mulloy [9] have noted that the phase angle, $\Phi$, depends on the atom numbering, i.e., ordering, used. We routinely use the order C-4–C-3–C-2–C-1–O-5–C-5–(C-6), determined by the directionality of the ring heavy atom sequence in the force field that we use. Forster and Mulloy [9] used the sequence O-5–C-1–C-2–C-3–C-4–C-5, whereas Ragazzi et al. [3] made use of the sequence C-1–C-2–C-3–C-4–C-5–O-5. For comparative purposes, therefore, we also report our $\Phi$ values for the two skew forms using both of these alternative nomenclatures.

The distorted inverted boat, the most stable of the two forms, has values of $\Phi_{(O\text{-}5\text{-}C\text{-}1\text{-}C\text{-}2\text{-}C\text{-}3\text{-}C\text{-}4\text{-}C\text{-}5)} = 90°$ and $\Phi_{(C\text{-}1\text{-}C\text{-}2\text{-}C\text{-}3\text{-}C\text{-}4\text{-}C\text{-}5\text{-}O\text{-}5)} = 30°$, clearly corresponding to the $^5S_1$ form. The second, less stable, skew form has values of $\Phi_{(O\text{-}5\text{-}C\text{-}1\text{-}C\text{-}2\text{-}C\text{-}3\text{-}C\text{-}4\text{-}C\text{-}5)} = 329°$ and $\Phi_{(C\text{-}1\text{-}C\text{-}2\text{-}C\text{-}3\text{-}C\text{-}4\text{-}C\text{-}5\text{-}O\text{-}5)} = 89°$, corresponding to the $^OS_2$ conformation, the inverse of that established for the iduronate ring, i.e., with $\Phi$ exactly 180° out of phase.

Unfortunately we have been unable to determine the $^3J_{HH}$ coupling constants for the Gal24N ring protons with any accuracy, because of poor spectral resolution, even using such editing techniques as 1D-TOCSY. Resolution of these protons is not adequate at 500 MHz for the native oligomer as a result of chemical-shift differences of the order of

Table 3
Torsional angles and inter-proton distances for the skew and chair forms of the Gal24N ring as described in the text

| | Ring torsions | | | | | | Inter-proton distances | | |
|---|---|---|---|---|---|---|---|---|---|
| | tor1 | tor2 | tor3 | tor4 | tor5 | tor6 | H-3–H-4 | H-3–H-5 | H-4–H-5 |
| $^5S_1$ skew | −62.4 | −30.9 | −23.8 | +53.9 | −23.6 | −33.3 | 2.24 (1.0) | 4.17 (1.86) | 2.37 (1.06) |
| $^4C_1$ chair | +57.2 | −57.0 | +55.9 | −55.7 | +59.8 | −60.2 | 2.47 (1.0) | 2.53 (1.04) | 2.43 (0.98) |

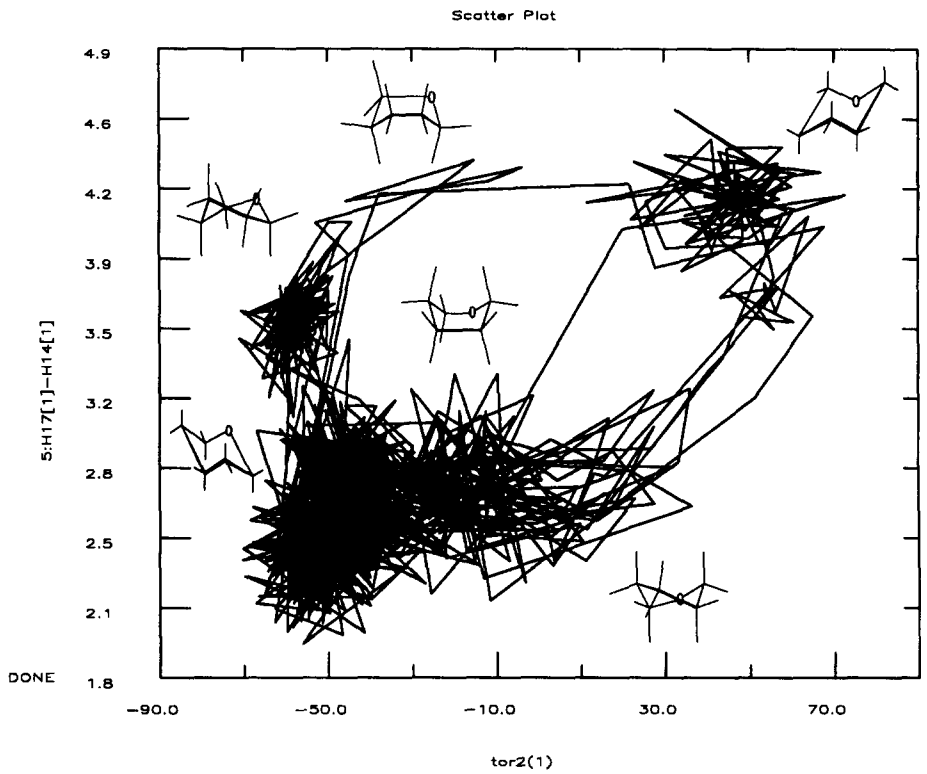


Fig. 4. A plot of tor2 (C-1–C-2–C-3–C-4) against the inter-proton distance H-3–H-5 for the 2,4,6-trideoxy-galactopyranose ring illustrating its use for determining ring conformation, as described in the text.

0.001 ppm and overlapping for the 5–7 Gal24N residues present. These coupling constants must be determined in the native oligomer, or in a derivative containing most of the functional components. Neither the per-*N*-acetylated oligomer nor the isolated

Fig. 5. (A) The ring torsion tor2 (C-1–C-2–C-3–C-4) plotted against the H-3–H-5 distance for partial trisaccharide (I), Me-β-D-glucose6P-(1 → 3)-2,4-diacetamido-2,4,6-trideoxy-α-D-galactose-[6-PC]-(1 → 4)-*N*-acetyl-α-D-galactosamine. (B) The histogram showing the distribution of the H-3–H-5 distance for partial trisaccharide (I), Me-β-D-glucose6P-(1 → 3)-2,4-diacetamido-2,4,6-trideoxy-α-D-galactose-[6-PC]-(1 → 4)-*N*-acetyl-α-D-galactosamine.

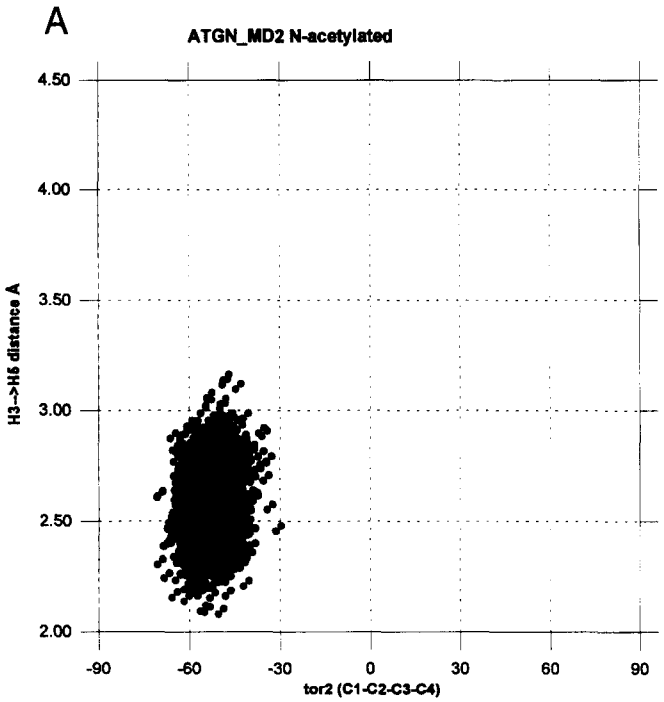
A
ATGN_MD2 N-acetylated
4.50
4.00
3.50
3.00
2.50
2.00
H3-->H5 distance Å
-90
-60
-30
0
30
60
90
tor2 (C1-C2-C3-C4)

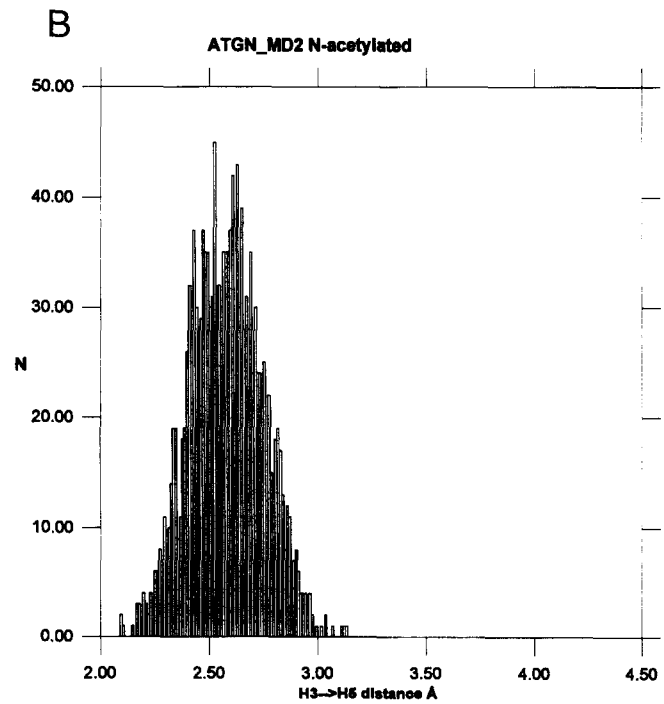
B
ATGN_MD2 N-acetylated
50.00
40.00
30.00
20.00
10.00
0.00
N
2.00
2.50
3.00
3.50
4.00
4.50
H3-->H5 distance Å

repeating-unit, both of which exhibit better spectral resolution, can be used, as the phosphate–amino group interaction is a prerequisite. We are currently working on preparing a derivative of the isolated repeating-unit that would be suitable for these measurements.

Calculation of the predicted $^3J_{HH}$ coupling constants, based on the data of Haasnoot et al. [23], show that the two pairs H-2–H-3 and H-3–H-4 would be the most sensitive to the difference in conformation between the chair and most stable skew form. The estimated values in Hz, with those for the $^4C_1$ galactopyranose ring in parentheses, are $^3J_{H\text{-}1,H\text{-}2} = 2.73$ (3.27); $^3J_{H\text{-}2,H\text{-}3} = 8.53$ (10.24); $^3J_{H\text{-}3,H\text{-}4} = 6.63$ (3.09); $^3J_{H\text{-}4,H\text{-}5} = 3.35$ (3.14).

The calculated relative stability of the distorted inverted boat, the $^5S_1$ conformer, is in keeping with the experimental NOE data discussed elsewhere in the text and with the evidence for interaction between the 4-amino and phosphate groups. The two most stable forms, the $^5S_1$ boat and $^4C_1$ chair, have the torsional angles and inter-proton distances shown in Table 3, with the torsional angles for the ring as defined previously.

MD simulations were carried out at 300 K for the three slightly different partial trisaccharide fragments: (i) Me-β-D-glucose6P-(1 → 3)-2,4-diacetamido-2,4,6-trideoxy-α-D-galactose-[6-PC]-(1 → 4)-*N*-acetyl-α-D-galactosamine (I); (ii) Me-β-D-glucose6P-(1 → 3)-2-acetamido-4-amino-2,4,6-trideoxy-α-D-galactose-[6-PC]-(1 → 4)-*N*-acetyl-α-D-galactosamine (II); and (iii) β-D-glucose-(1 → 3)-2-acetamido-4-amino-2,4,6-trideoxy-α-D-galactose-[6-PC]-(1 → 4)-*N*-acetyl-α-D-galactosamine (III).

We have used plots of the ring torsion tor2 (C-1–C-2–C-3–C-4) against the H-3–H-5 distance as a means of exploring ring conformational space for the Gal24N. The usefulness of this method is shown diagrammatically in Fig. 4, in which drawings of various ring conformations have been superimposed on the results of a long-term MD simulation for an isolated 2,4,6-trideoxy-galactopyranose ring at 1000 K, used merely as an example. Different ring geometries correspond to different combinations of tor2 and H-3–H-5, located on an ellipse with the major axis represented at either end by the $^4C_1$ and $^1C_4$ chair conformations respectively.

Results from the MD simulation for the per-*N*-acetylated trisaccharide (I) are shown in Fig. 5A (tor2 against H-3–H-5 distance) and in Fig. 5B (the H-3–H-5 distance histogram). Analogous results for the trisaccharide with a free 4-$NH_2$ group (II) and without the 6-phosphate methyl ester (III), are shown in Fig. 6A and 6B, and in Fig. 7A and 7B.

All of these MD simulations were started using ring geometries that were either boat or skew. As discussed by Forster and Mulloy [9] in their MD study of the conformation of the iduronate ring, starting with chair geometries gave trajectories which only showed ring oscillations close to the initial geometry. This is almost certainly due to the relatively high activation energy needed to pass from the chair to boat/skew conforma-

Fig. 6. (A) The ring torsion tor2 (C-1–C-2–C-3–C-4) plotted against the H-3–H-5 distance for partial trisaccharide (II), Me-β-D-glucose6P-(1 → 3)-2-acetamido-4-amino-2,4,6-trideoxy-α-D-galactose-[6-PC]-(1 → 4)-*N*-acetyl-α-D-galactosamine. (B) The histogram showing the distribution of the H-3–H-5 distance for partial trisaccharide (II), Me-β-D-glucose6P-(1 → 3)-2-acetamido-4-amino-2,4,6-trideoxy-α-D-galactose-[6-PC]-(1 → 4)-*N*-acetyl-α-D-galactosamine.

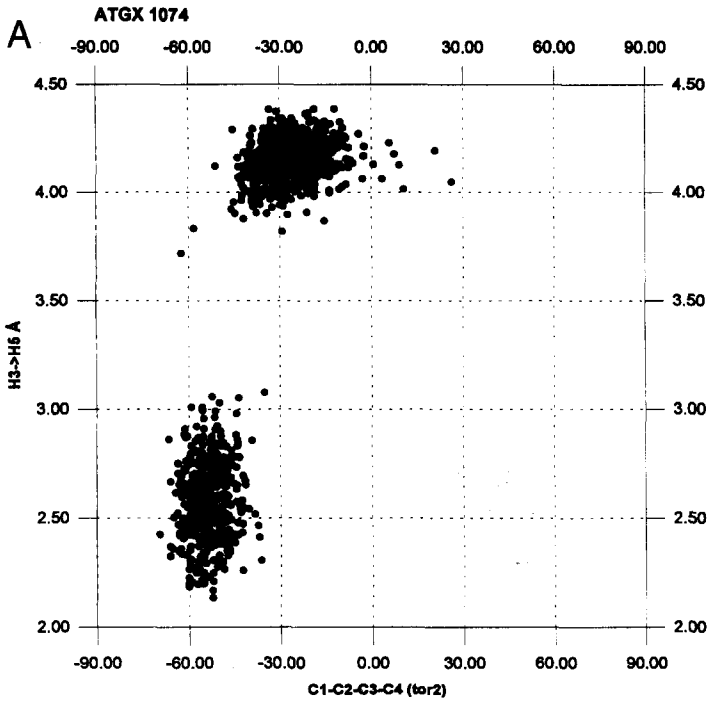
A
ATGX 1074
-90.00
-60.00
-30.00
0.00
30.00
60.00
90.00
4.50
4.00
3.50
3.00
2.50
2.00
H3->H6 A
C1-C2-C3-C4 (tor2)

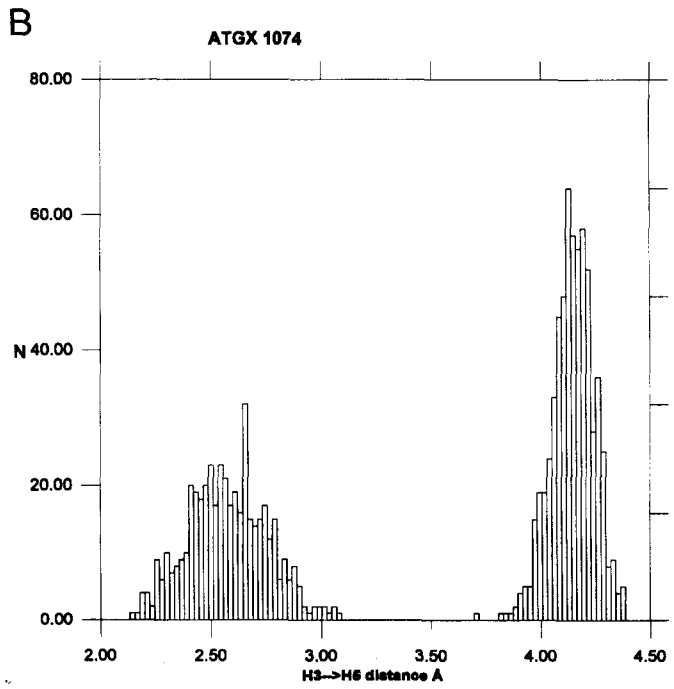
B
ATGX 1074
80.00
60.00
N 40.00
20.00
0.00
2.00
2.50
3.00
3.50
4.00
4.50
H3-->H6 distance A

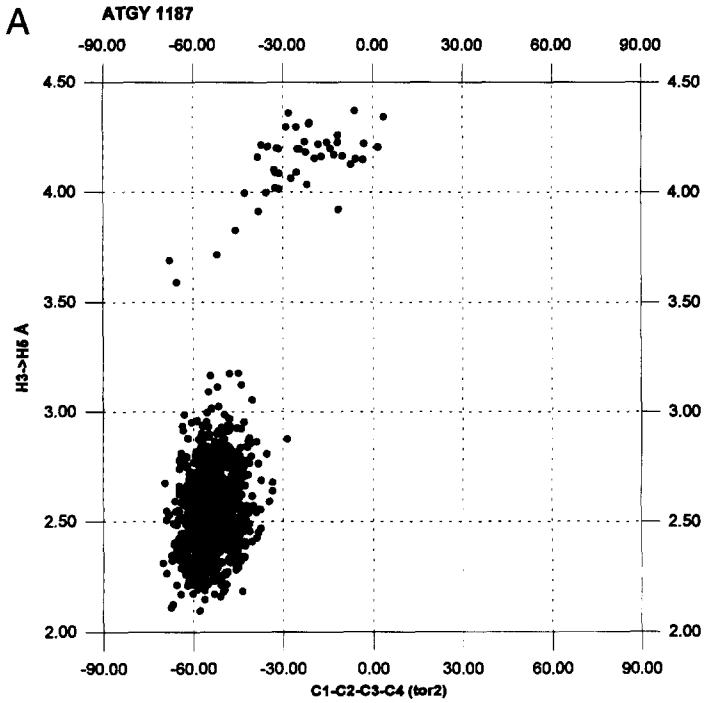
A
ATGY 1187
-90.00
-60.00
-30.00
0.00
30.00
60.00
90.00
4.50
4.00
3.50
3.00
2.50
2.00
H3->H6 Å
C1-C2-C3-C4 (tor2)

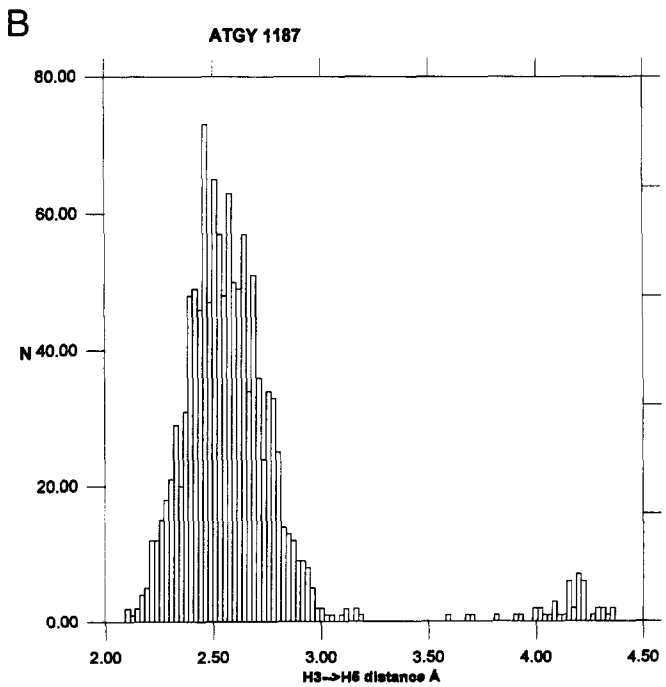
B
ATGY 1187
80.00
60.00
N 40.00
20.00
0.00
2.00
2.50
3.00
3.50
4.00
4.50
H3-->H6 distance Å

tion, especially if the MD simulation is not done at elevated temperatures, for example 1000 K. Based on our results, we would estimate the barrier to be of the order of 10–15 kcal/mol for this transition, sufficient for the process to be considered almost irreversible at 300 K.

The data shown in Figs. 5–7 indicate that, whereas the per-*N*-acetylated Gal24N ring adopts the $^4C_1$ chair geometry to the exclusion of other conformers, as in compound (I), the presence of a free 4-$NH_2$ group, as in (II), results in an approximately equal population of $^4C_1$ chair and $^5S_1$ skew conformers. Removal of the 6-phosphate group, as in (III), results in re-establishment of the conformational preference for the $^4C_1$ chair. Clearly the interaction between the free amino group and the phosphate group is central for the conformational change in the 2,4,6-trideoxy-galactopyranose ring. All of these MD simulations were started from a skew or inverted boat geometry. The per-*N*-acetylated trisaccharide always passed very rapidly into the $^4C_1$ chair conformation, usually within 1–2 ps at 300 K, whereas even trisaccharide (III), containing Gal24N with a free 4-amino group but no phosphate 6-linked to the glucose, resided for some time in the starting geometry, although to a much lesser extent than trisaccharide (II). Mention has already been made of Forster and Mulloy's comments on starting geometry in these type of MD simulations [9]. One might reasonably expect to see some "residual" $^5S_1/B_{1,4}$ stability of the 4-amino Gal24N pyranose ring, as in trisaccharide (II), in spite of the absence of the amino–phosphate interaction, in comparison with the per-*N*-acetylated material. Rapid interchange was observed in MD simulations between these forms, representing movement of about 30° in the value of $\Phi$ around the Cremer–Pople equator.

The calculated conformation of the (1 → 3) glycosidic linkage between the β-D-glucose and the α-D-Gal24N residues appears to be affected by the presence (II) or absence (I) of this interaction between the amino and phosphate groups. In the per-acetylated derivative (I) $\Phi = +130°$ and $\Psi = -48°$ with H-1–H-3 = 3.27 Å; in the derivative with a free 4-$NH_2$ group (II), these values are $\Phi = +57°$ and $\Psi = -7°$ with H-1–H-3 = 2.34 Å. Our experimental NOE results indicate that the force field may be overestimating the strength of the interaction as the difference in inter-proton distances, judged from the NOE cross-peak intensities, is not as great as calculated. Experimentally determined values for the $A_{H\text{-}1}$–$B_{H\text{-}3}$ distance are virtually the same for the native and acetylated oligomer (2.48 ± 0.03 Å compared to 2.50 ± 0.02 Å), suggesting either that the force field overestimates the interaction or that the terminal glucose residue is much less mobile within the oligomer chain than in the partial trisaccharide, the second being the most likely. This point will be dealt with in greater detail in another paper concerned with the conformation of the glycosidic linkages in the intact oligomer.

Fig. 7. (A) The ring torsion tor2 (C-1–C-2–C-3–C-4) plotted against the H-3–H-5 distance for partial trisaccharide (III), β-D-glucose-(1 → 3)-2-acetamido-4-amino-2,4,6-trideoxy-α-D-galactose-[6-PC]-(1 → 4)-*N*-acetyl-α-D-galactosamine. (B) The histogram showing the distribution of the H-3–H-5 distance for partial trisaccharide (III), β-D-glucose-(1 → 3)-2-acetamido-4-amino-2,4,6-trideoxy-α-D-galactose-[6-PC]-(1 → 4)-*N*-acetyl-α-D-galactosamine.

## 4. Conclusions

We have demonstrated, using $^{31}$P- and $^{1}$H-NMR methods together with computer modelling, that the galactopyranose ring of the Gal24N residue in *Streptococcus pneumoniae* lipoteichoic acid can adopt a conformation in aqueous solution other than the usual $^{4}C_{1}$ chair. The biological significance of this conformational mobility of the galactopyranose ring is not clear, although it may be important for the specificity of any antibody response and the expression of antigenicity. The change in conformation is associated with an interaction between the negatively charged phosphate group and the positively charged amino group, as well as hydrogen bonding to the glucose ring oxygen, which results in the 4-$NH_2$ group being equatorial rather than axial, as is normally the case for $^{4}C_{1}$ Gal24N.

Interestingly, the charged capsular polysaccharides A and B from *Bacteroides fragilis* appear to require the presence of oppositely charged groups in order to induce abscess formation in the rat model [24–26]. Both polysaccharides contain Gal24N. It is tempting to speculate that the biological activity, in this case abscess formation, is not associated per se with the presence of oppositely charged groups but rather with the conformational change associated with them and induced in the Gal24N hexopyranose ring. This alteration in molecular conformation in turn could modulate the expression of antigenicity and the ability of the capsular polysaccharide to stimulate a T cell-dependent response (see references in ref. [26]). Conformational changes in the sugar ring would profoundly affect the three-dimensional hydroxyl surface "seen" by antibodies or other cell-surface receptors, as well as bringing about changes in the structured water within the solvation shell through hydrogen bonding and electrostatic field effects. Such conformational changes could represent an additional mechanism in the biological repertoire for expressing epitope immunogenicity.

In all our calculations water was implicitly included using a distance-dependent dielectric constant. Explicit inclusion of TIP3 water molecules, with imaging, was too CPU intensive to be useful in the present instance. The nuclear Overhauser effect data suggest that the skew conformation for the Gal24N ring is more highly populated than indicated by the MD simulation results. The average NOE-derived distance for the H-3–H-5 pair is $3.1 \pm 0.3$ Å, indicating a population distribution of approximately 30:70% in favour of the skewed boat. The data shown in Fig. 6B points to a 60:40% distribution in the other direction. There are two possible reasons for this quantitative discrepancy. As mentioned previously, the conformational equilibrium may not be, in practice at least, reversible at relatively low temperatures, because of the high activation energy required for $^{4}C_{1} \Rightarrow {}^{5}S_{1}$, resulting in an unrealistic distribution. This situation may be improved by conducting the simulation at 1000 K (results not shown).

Secondly, the modelling of solvent water using the implicit distance-dependent dielectric constant method may fail to reproduce the correct distribution of conformers, as only slight energy differences would be needed. We have recently shown, however, that the CHARMm force field, together with Gasteiger charges, performs reasonably well with permanently charged oligosaccharides containing neuraminic acid residues in aqueous solution, as judged from experimental NOE data [27].

We are currently assessing the use of an extended atom approach for the sugar

hydroxyl groups and their hydrogen-bonding interactions in modelling the lipoteichoic acids (Carbohydrate Extended Atom—CHEAT: Grootenhuis et al. [28]). A subsequent paper will deal with this aspect as well as the effects of the Gal24N conformational equilibrium on the conformation of the inter-residue glycosidic backbone in the intact LTA oligomer.

The structure of the repeat unit in the C-polysaccharide from *S. pneumoniae* R36A and in the lipoteichoic acid (LTA) from *S. pneumoniae* R6 are identical [1,29]. Indications that a conformational change was associated with *N*-acetylation, based on chemical shift displacements, were reported in a much earlier paper from the same group [30], in which it was suggested that "... bonds vicinal to residue B [Gal24N] are the most affected by the *N*-acetylation of PnC [the repeat unit] ...". Our results provide a detailed molecular explanation for this earlier observation based on NMR chemical shift data.

## Acknowledgements

We should like to acknowledge financial support in the form of a program grant from the Deutsche Forschungsgemeinschaft (DFG SFB 284/A1).

## References

[1] R.A. Klein, R. Hartmann, H. Egge, T. Behr, and W. Fischer, *Carbohydr. Res.*, 256 (1994) 189–222.
[2] G. Torri, B. Casu, G. Gatti, M. Petitou, J. Choay, J.C. Jacquinet, and P. Sinaÿ, *Biochem. Biophys. Res. Commun.*, 128 (1985) 134–140.
[3] M. Ragazzi, D.R. Ferro, and A. Provasoli, *J. Comput. Chem.*, 7 (1986) 105–112.
[4] M. Ragazzi, D.R. Ferro, B. Perly, G. Torri, B. Casu, P. Sinaÿ, M. Petitou, and J. Choay, *Carbohydr. Res.*, 165 (1987) c1–c5.
[5] B. Casu, M. Petitou, M. Provasoli, and P. Sinaÿ, *Trends Biochem. Sci.*, 13 (1988) 221–225.
[6] D.R. Ferro, A. Provasoli, M. Ragazzi, B. Casu, G. Torri, V. Bossennec, B. Perly, P. Sinaÿ, M. Petitou, and J. Choay, *Carbohydr. Res.*, 195 (1990) 157–167.
[7] M. Ragazzi, D.R. Ferro, B. Perly, P. Sinaÿ, M. Petitou, and J. Choay, *Carbohydr. Res.*, 195 (1990) 169–185.
[8] L. Kjellen and U. Lindahl, *Ann. Rev. Biochem.*, 60 (1991) 443–475.
[9] M.J. Forster and B. Mulloy, *Biopolym.*, 33 (1993) 575–588.
[10] P.L. Durette and D. Horton, *Adv. Carbohydr. Biochem.*, 26 (1971) 49–125.
[11] C. Altona and C.A.G. Hasnoot, *Org. Magn. Reson.*, 13 (1980) 417–429.
[12] T. Behr, W. Fischer, J. Peter-Katalinic, and H. Egge, *Eur. J. Biochem.*, 207 (1992) 1063–1075.
[13] S. Macura and R.R. Ernst, *Mol. Phys.* 41 (1980) 95–117.
[14] A. Kumar, G. Wagner, R.R. Ernst, and K. Wütrich, *J. Am. Chem. Soc.*, 103 (1981) 3654–3658.
[15] F. Longchambon, D.A. Ohannessian, and A. Neuman, *Acta Crystallogr., Sect B*, 31 (1975) 2623–2627.
[16] B. Sheldrick, *Acta Crystallogr., Sect B*, 32 (1976) 1016–1020.
[17] J.N. Scarsdale, J.H. Prestegard, and R.K. Yu, *Biochemistry*, 29 (1990) 9843–9855.
[18] B.R. Brooks, R.E. Bruccoleri, B.D. Olafson, D.J. States, S. Swaminathan, and M. Karplus, *J. Comput. Chem.*, 4 (1983) 187–217.
[19] J. Gasteiger and M. Marsili, *Tetrahedron*, 36 (1980) 3219–3228.
[20] E.L. Eliel, *Stereochemistry of Carbon Compounds*, McGraw-Hill, New York, 1962.
[21] D. Cremer and J.A. Pople, *J. Am. Chem. Soc.*, 97 (1975) 1354–1358.

[22] J.F. Stoddart, *The Stereochemistry of Carbohydrates*, Wiley, New York, 1971.
[23] C.A.G. Haasnoot, F.A.A.M. de Leeuw, and C. Altona, *Tetrahedron*, 36 (1980) 2783–2792.
[24] A.O. Tzianabos, A. Pantosti, H. Baumann, J.-R. Brisson, H.J. Jennings, and D.L. Kasper, *J. Biol. Chem.*, 267 (1992) 18230–18235.
[25] H. Baumann, A.O. Tzianabos, J.-R. Brisson, D.L. Kasper, and H.J. Jennings, *Biochemistry*, 31 (1992) 4081–4089.
[26] A.O. Tzianabos, A.B. Onderdonk, B. Rosner, R.L. Cisneros, and D.L. Kasper, *Science*, 262 (1993) 416–419.
[27] R.A. Klein, D. Machytka, G. Sirch, and H. Egge, *Carbohydr. Res.*, submitted for publication.
[28] P.D.J. Grootenhuis and C.A.G. Hasnoot, *Mol. Simul.*, 10 (1993) 75–95.
[29] M. Kulakowska, J.-R. Brisson, D.W. Griffith, N.M., Young, and H.R. Jennings, *Can. J. Chem.*, 71 (1993) 644–648.
[30] H.R. Jennings, C. Lugowski, and N.M. Young, *Biochemistry*, 19 (1980) 4712–4719.